Brazilian Journal
of Chemical
Engineering

ISSN 0104-6632
Printed in Brazil
www.abeq.org.br/bjche

Vol. 32, No. 01, pp. 303 - 316, January - March, 2015
dx.doi.org/10.1590/0104-6632.20150321s00003120

THERMOPHYSICAL PROPERTIES OF 1-BUTYL-3-METHYLIMIDAZOLIUM BIS(TRIFLUOROMETHYLSULFONYL)IMIDE AT HIGH TEMPERATURES AND PRESSURES

R. Hamidova[1], I. Kul[2], J. Safarov[1,3*], A. Shahverdiyev[1] and E. Hassel[3]

[1]Department of Heat and Refrigeration Techniques, Azerbaijan Technical University, H. Javid Avn. 25, AZ1073, Baku, Azerbaijan.
[2]Department of Chemistry and Biochemistry, Widener University, One University Place, Chester, PA 19013, USA.
[3]Institute of Technical Thermodynamics, University of Rostock, Albert-Einstein-Str. 2, D-18059 Rostock, Germany.
Phone: + 49 381 4989415, Fax:+ 49 381 4989402
E-mail: javid.safarov@uni-rostock.de

(Submitted: November 13, 2013 ; Revised: May 13, 2014 ; Accepted: May 19, 2014)

Abstract - Pressure-density-temperature (p,ρ,T) data of the ionic liquid 1-butyl-3-methylimidazolium bis(trifluoromethylsulfonyl)imide [BMIM][NTf_2] at T = (273.15 to 413.15) K and pressures up to p =140 MPa are reported with an estimated experimental relative combined standard uncertainty of $\Delta\rho/\rho = \pm$(0.01 to 0.08)% in density. The measurements were carried out with a newly constructed Anton-Paar DMA HPM vibration-tube densimeter. The system was calibrated using double-distilled water, aqueous NaCl solution, methanol, toluene and acetone. An empirical equation of state for fitting the (p,ρ,T) data of [BMIM][NTf_2] has been developed as a function of pressure and temperature. This equation is used for the calculation of the thermophysical properties of the ionic liquid, such as isothermal compressibility, isobaric thermal expansibility, thermal pressure coefficient, internal pressure, isobaric and isochoric heat capacities, speed of sound and isentropic expansibility.
Keywords: Density; Vibration tube densimeter; Equation of state; Isothermal compressibility; Isobaric thermal expansibility.

INTRODUCTION

Ionic liquids (ILs) are salts that are in liquid state at low temperature (<100 °C) and they are non-flammable, thermally stable and have no detectable vapor pressure. They are excellent solvents for a broad range of polar organic compounds and they show partial miscibility with aromatic hydrocarbons. Thus, they are under intense investigation, especially as replacement solvents for reactions and separations. In addition, because of their chemical and physical properties, there are useful applications for them within several disciplines such as in synthetic chemistry, sensors, solar cells, solid-state photocells and batteries and as thermal fluids, lubricants, and hydraulic fluids, to name only a few (Wu *et al*., 2001; Valkenburg *et al*., 2005; Kim *et al*., 2003; Dupont, 2004; Handy, 2011).

This work is a continuation of our investigations in the field of thermophysical properties of ionic liquids (Safarov *et al*., 2013). Included are the (p,ρ,T) properties of [BMIM][NTf_2] at T = (273.15 to 413.15) K and at pressures up to p = 140 MPa, measured for the first time over such wide temperature and pressure intervals using a vibrating tube densimeter. The thermophysical properties [isothermal compressibility $\kappa_T(p,T)$/MPa^{-1}, isobaric thermal expansibility $\alpha_p(p,T)$/K^{-1}, thermal pressure coefficient $\gamma(p,T)$/MPa·K^{-1}, inter-

*To whom correspondence should be addressed

nal pressure $p_{int}(p,T)$/MPa, specific heat capacities $c_p(p,T)$/J·kg^{-1}·K^{-1} and $c_v(p,T)$/J·kg^{-1}·K^{-1}, speed of sound $u(p,T)$/m·s^{-1}, isentropic expansibilities $\kappa_s(p,T)$] were calculated at high pressures and temperatures, in which the density of [BMIM][NTf$_2$] was measured.

The first density data of [BMIM][NTf$_2$] were measured at T = 298.15 K by a simple gravimetric analysis using 1 mL by pipette and the average density data was reported by Huddleston *et al.* (2001).

Krummen *et al.,* (2002) measured the density ρ/kg·m^{-3} of [BMIM][NTf$_2$] as a function of temperature between T = (293.15 and 353.15) K at ambient pressure using the Anton Paar vibrating tube densimeter to determine activity coefficients at infinite dilution in ionic liquids.

Holbrey *et al.*, (2003) investigated the heat capacity values of [BMIM][NTf$_2$] at T = (293.1 to 453.1) K.

Fredlake *et al.*, (2004) studied thermophysical properties of [BMIM][NTf$_2$], including melting temperature, glass-transition temperature, decomposition temperature, heat capacity as a function of temperature, and density ρ/kg·m^{-3} of [BMIM][NTf$_2$] at T=(296.15 to 333.75) K and ambient pressure using a 1 mL pycnometer.

Tokuda *et al.*, (2005) measured the density ρ/kg·m^{-3} of [BMIM][NTf$_2$] at T = (288.15 and 313.15) K using a thermoregulated DA-100 density/specific gravity meter. The linear dependence of density versus temperature was developed and fitting parameters of this dependence were presented.

Speed of propagation of ultrasound waves u/m·s^{-1} and densities of [BMIM][NTf$_2$] at T = (298.15 to 328.15) K and pressures up to 59.10 MPa have been determined by de Azevedo *et al.* (2005) using an Anton Paar DMA 60 digital vibrating tube densimeter, with a DMA 512P measuring cell. These are the first (p,ρ,T) measurements of [BMIM][NTf$_2$]. The Tait equation without coefficient dependence on temperature was used for fitting of the measured values to calculate the thermal properties of the IL.

Bagno *et al.* (2005) measured some of the thermophysical properties, including density, conductivity, melting point, refractive index, surface tension and diffusion coefficient of [BMIM][NTf$_2$] at T = 298.15 K. The densities of [BMIM][NTf$_2$] were determined by gravimetric analysis by measuring the weight of the sample in a 1 cm^3 calibrated flask.

Jacquemin *et al.* (2006) measured the density ρ/kg·m^{-3} of [BMIM][NTf$_2$] at T = (292.88 to 391.28) K using a U-shape vibrating-tube densimeter (Anton Paar, model DMA 512) operating in a static mode. The precision of the density measurement was 10^{-4} g·cm^{-3} and the results were expected to be accurate to 10^{-3} g·cm^{-3}.

Tokuda *et al.* (2006) presented values of density ρ/kg·m^{-3} of [BMIM][NTf$_2$] at T = (288.15 to 313.15) K and ambient pressure using a thermo-regulated density/specific gravity meter DA-100 (Kyoto Electronics Manufacturing Co. Ltd.).

Troncoso *et al.* (2006) reported the experimental densities ρ/kg·m^{-3}, isobaric heat capacities c_p/J·mol^{-1}·K^{-1}, and enthalpies of fusion of two different samples of [BMIM][NTf$_2$] at atmospheric pressure. The density and the heat capacity measurements were in the T = (278.15 to 333.15) K temperature interval using a DMA-5000 vibrating-tube densimeter from Anton-Paar. Calibration was performed using Milli-Q water and dry air as density standards. A critical analysis of the effect of impurities on the measured thermodynamic properties was performed. The estimated uncertainty was $\pm 1\cdot10^{-5}$ g·cm^{-3}. Isobaric molar heat capacities c_p were obtained using a Micro DSCII differential scanning calorimeter from Setaram. The scanning method at a rate of 0.25 K·min^{-1} was used. The uncertainty in c_p for commonly used, high-purity organic solvents is estimated to be $\pm$0.2 J·mol^{-1}·K^{-1}.

Jacquemin *et al.* (2007) investigated the densities ρ/kg·m^{-3} of [BMIM][NTf$_2$] as a function of temperature at T=(293.49 to 414.92) K and over an extended pressure range at p = (0.1 to 40) MPa using a vibrating tube densimeter (Anton Paar, DMA 512). The uncertainty of the density measurement was $\pm 1\cdot10^{-4}$ g·cm^{-3}.

Harris *et al.* (2007) investigated the viscosities η/mPa·s of [BMIM][NTf$_2$] between T = (273.15 to 353.15) K and at maximum pressures of 300 MPa with a falling body viscometer. The viscosity calculations were performed using density data reported by de Azevedo *et al.* (2005). These values were fitted to the Hayward-type equation for the extrapolation of the density values up to the experimental temperature and pressure interval of the measured viscosity values.

Shimizu *et al.* (2008) studied the heat capacity of [BMIM][NTf$_2$] at T = (250 to 300) K using adiabatic calorimetry and they observed a broad heat capacity anomaly and spontaneous endothermic effect for the crystal phase. The relation between these anomalies and thermal history after crystallization was described.

Wandschneider *et al.* (2008) used the pendant drop method for measuring the surface tension σ/n·m^{-1} of [BMIM][NTf$_2$] at T = (292.88 to 391.28) K. The required density ρ/kg·m^{-3} data of IL were obtained using a vibrating tube densimeter (Anton Paar DMA 512 P), which was calibrated at each temperature using liquid water, dry air, and *n*-hexane as calibration substances. The uncertainty of the density data was estimated to be $\pm 1\cdot10^{-4}$ g·cm^{-3}.

Ge *et al.* (2008) investigated the heat capacity c_p/J·mol^{-1}·K^{-1} of [BMIM][NTf$_2$] as a function of temperature between 293 K to 358 K by using a heat flux differential scanning calorimeter (model DSC Q100) with an uncertainty of 5%.

Blokhin *et al.* (2008) investigated the thermodynamic properties of [BMIM][NTf$_2$] using adiabatic calorimetry in the temperature range of T = (5 to 370) K. The measurements were conducted in a Termis TAU-10 adiabatic calorimeter. The maximum error of the measurements did not exceed $\pm 4 \cdot 10^{-3}$ c_p in the range of T = (20 to 370) K, $\pm 1 \cdot 10^{-2}$ c_p at T = (10 to 20) K, and $\pm 2 \cdot 10^{-2}$ c_p at T < 10 K.

Katsuta *et al.* (2010) studied the various thermophysical properties of [BMIM][NTf$_2$]: melting points by the rising melting point method using a thermocontrolled water bath and a primary standard thermometer; densities at T = (293.2 to 308.4) K using an oscillating U-tube density meter (Anton Paar, DMA35n); kinematic viscosities at T = (292.5 to 308.7) K using an Ubbelohde-type viscometer (KUSANO, No. 2); electric conductivities with a digital conductimeter (TOA Electrics, CM-40S).

Geppert-Rybczyńska *et al.* (2010) studied the densities of pure as well as six binary mixtures containing the ionic liquid 1-butyl-3-methylimidazolium bis(trifluoromethylsulfonyl)imide mixed with tetrahydrofuran or acetonitrile or dimethyl sulfoxide at atmospheric pressures in the temperature range between T = (293.15 K and 313.15) K using a vibrating-tube densimeter (model Anton Paar DMA 602) to determine excess molar volumes of solutions.

Vranes *et al.* (2012) studied the density of [BMIM][NTf$_2$] at T = (293.15 K and 353.15) K and, from these values, the thermal expansion coefficient was calculated. In addition, the specific conductivity of the IL was measured in the range from T = (303.15 to 353.15) K and viscosity of the IL was measured from room temperature up to T = 353.15 K. The temperature effect on the viscosity was analyzed by using the obtained experimental data.

Analysis of the literature (Table 1) shows the necessity of careful experimental (p,ρ,T) measurement of [BMIM][NTf$_2$] over a wide range of temperatures and pressures, including temperatures below ambient temperature and at high pressures for the following reasons:

- There are no density values above p = 59.10 MPa;
- There are only a few thermophysical properties and these are within the small interval range;
- Only the Tait equation is used for fitting of (p,ρ,T) properties (de Azevedo *et al.*, 2005; Jacquemin *et al.*, 2007);
- The literature values have large deviations between them (up to $\Delta\rho/\rho = \pm 1\%$).

In our case the (p,ρ,T) properties of [BMIM][NTf$_2$] at T = (273.15 to 413.15) K and at pressures p = (0.101 to 140) MPa are measured using a high pressure – high temperature vibrating tube densimeter. Densities of [BMIM][NTf$_2$] at ambient pressure and at temperatures T = (278.15 to 343.15) K are also measured using an Anton-Paar DSA 5000M vibrating tube densimeter and sound velocity meter.

EXPERIMENTAL

The (p,ρ,T) measurements were carried out using a new modernized high pressure – high temperature Anton-Paar DMA HPM vibrating tube densimeter [Safarov *et al.*, (2009), Guliyev *et al.*, (2009)]. Density measurements with a vibrating tube are based on the dependence of the period of oscillation of a unilaterally fixed U - tube (Hastelloy C - 276) on its mass. This mass consists of the U - tube material and the mass of the fluid filled into the U - tube.

The temperature in the measuring cell where the U – tube is located is controlled using a thermostat (F32 - ME Julabo, Germany) with an error of ±10 mK and is measured using an (ITS-90) Pt100 thermometer (Type 2141) with an experimental error of ±15 mK. Pressure is measured by P-10 and HP-1 pressure transmitters (WIKA Alexander Wiegand GmbH & Co., Germany) with a relative uncertainty of (0.1 and 0.5)% respectively, of the measured value.

The sample in the oscillating tube is part of a complex system. The force of inertial shear forces occurs on the wall, influencing the resonant frequency of the oscillator. If samples of higher viscosities are measured, one notices that the displayed density is too high. Up to a certain level, this error is a function of viscosity [Aschcroft *et al.*, (1990) and Stabinger, (1994)]. The behavior can be explained by considering a segment of the oscillator in motion. Investigating a "slice" of sample one finds that both translational and rotational movements take place. The force required to keep the slice rotating is introduced by shear forces on the wall. As the viscosity increases, an increasing part will rotate until the whole slice rotates like a solid body. The momentum of inertia of the rotated section, when added to the force of inertia of the movement of translation, simulates a higher mass with respect to volume, and so a higher density. A correction can easily be performed if the form of the error curve and the sample viscosity are known [Aschcroft *et al.*, (1990), Stabinger, (1994) and Fitzgerald, (1992)].

Table 1: Summary of the density measurements for [BMIM][NTf_2].

Source	Method	Properties	Temperature, T/K	Pressure, p/MPa	Uncertainty, $\Delta\rho$	Fitted density equation	Purity	Company of Purchase
Huddleston *et al*. (2001)	GA	ρ, T	298.15	0.101	NA		115 ppm	LP
Krummen *et al*. (2002)	VTD	ρ, T	293.15 to 353.15	0.101	$\pm1\cdot10^{-4}$ g·cm^{-3}		100 ppm	LP
Holbrey *et al*. (2003)		c_p	293.1 to 453.1	0.101				
Fredlake *et al*. (2004)	PC	ρ, T, c_p, T_m, T_f, T_{cc}, T_g	296.15 to 333.75	0.101	NA		460 ppm	Covalent Associates, Inc.
de Azevedo *et al*. (2005)	VTD	p, ρ, T, κ_s, κ_T, α_p, γ, c_p, c_v, u	298.15 to 328.15	0.101 to 59.10	0.02%	Tait	75 ppm	LP, OUILL
Bagno *et al*. (2005)	GA	ρ, T	298.15	0.101	NA		NA	LP
Jacquemin *et al*. (2006)	VTD	ρ, T	292.88 to 391.28	0.101	$\pm1\cdot10^{-4}$ g·cm^{-3}		10^{-4} water m.f.	LP
Tokuda *et al*. (2006)	TRD	ρ, T	283.15 to 313.15	0.101	NA		NA	LP
Troncoso *et al*. (2006)	VTD, DSC	ρ, c_p,$\Delta_{fus}H$	278.75 to 333.15	0.101	$\pm1.5\cdot10^{-5}$ g·cm^{-3} (ρ) ±0.2 J·mol^{-1}·K^{-1} (c_p)		130 ppm 20 ppm	LP, OUILL, Covalent Associates, Inc.
Jacquemin *et al*. (2007)	VTD	p, ρ, T, κ_T, α_p,	293.49 to 414.92	0.101 to 40	$\pm1\cdot10^{-4}$ g·cm^{-3}	Tait	10^{-4} water m.f.	LP
Harris *et al*. (2007)	VTD	p, ρ, T,η	273.15 to 363.15	0.101 (ρ)	$\pm1\cdot10^{-5}$ g·cm^{-3}		$19\cdot10^{-6}$ water m.f.	LP
Shimizu *et al*. (2007)	AC	c_p	250 to 300	0.101				
Wandschneider *et al*. (2008)	VTD	σ, ρ, T	292.88 to 391.28	0.101	$\pm1\cdot10^{-4}$ g·cm^{-3}		$2.15\cdot10^{-4}$ water m.f.	LP
Ge *et al*. (2008)	DSC	c_p	293 to 358	0.101	5%		$96\cdot10^{-6}$ water m.f.	LP
Blokhin *et al*. (2008)	AC	c_p	5 to 370	0.101	$2\cdot10^{-2}$ c_p		0.985 m.f.	LP
Katsuta *et al*. (2010)	VTD	ρ, c_p, η	293.2 to 308.4	0.101	$\pm1\cdot10^{-3}$ g·cm^{-3}			
Geppert-Rybczyńska *et al*. (2010)	VTD	ρ	293.15 to 313.15	0.101	$\pm2\cdot10^{-5}$ g·cm^{-3}			
Vranes *et al*. (2012)	VTD	ρ	293.15 to 313.15	0.101	$\pm1\cdot10^{-5}$ g·cm^{-3}		99%	Merck AG

GA, gravimetric analysis; ρ, density; T, temperature; T_m, melting temperature; T_f, freezing temperature; T_{cc}, cold crystallization temperature; T_g, glass-transition temperature; NA, not available; LP, laboratory product; VTD, Vibrating tube densimeter; PC, Pycnometer; κ_s, isoentropic compressibility; κ_T, isothermal compressibility; α_p, isobaric thermal expansibility; γ, thermal pressure coefficient; c_p,heat capacity at constant pressure; c_v,heat capacity at constant volume; u. speed of sound; m.f., mass fraction; c_p,heat capacity; $\Delta_{fus}H$, enthalpy of fusion; DSC, differential scanning calorimeter; σ; surface tension; AC, adiabatic calorimetry

In the present work the viscosity correction $(\rho_{HPM}-\rho)/\rho_{HPM}$ (Segovia *et al*., 2009) was included in the density measurements as follows:

$$\frac{\rho_{HPM}-\rho}{\rho_{HPM}} = [0.4482\sqrt{\eta} - 0.1627]\cdot10^{-4}, \quad (1)$$

For evaluation of Eq. (1) we need $(\rho_{HPM}-\rho)/\rho_{HPM}$ as a function of viscosity η, which must be known in the same temperature and pressure range where densities are determined. For the determination of the dependence of this correction term on temperature and pressure, the viscosity values of [BMIM][NTf_2] of Harris *et al.* (2007) with an extrapolation to T = 273.15 K and p = 140 MPa were used.

The mPDS2000V3 control unit measures the vibration period with an accuracy of $\Delta\tau = \pm0.001$ μs. According to the specifications of Anton-Paar and the calibration procedures, the observed repeatability of the density measurements at temperatures T = (273.15 to 413.15) K and pressures up to p = 140 MPa was within $\Delta\rho$ = ±(0.1 to 0.3) kg·m^{-3} or $\Delta\rho/\rho$ = ±(0.01 to 0.03)%. The described uncertainty of the viscosity measurements in the literature and the application of those results to the temperature and pressure intervals of our work increase the possible uncertainty of the density measurements of the present work. From the other point of view, the effect of the right side of Eq. (1) is small and the uncertainty increase in the density correction is not very large. Thus, the uncertainty of the density measurements

can be predicted to be between $\Delta\rho = \pm(0.1 \text{ to } 0.8)$ kg·m^{-3} or $\Delta\rho/\rho = \pm$ (0.01 to 0.08)%.

The ionic liquid [BMIM][NTf_2] was purchased from EMD Chemicals Inc. (Merck Group), Germany (CAS No. 174899-83-3) with a purity ≥ 98.0%. To reduce the water content and volatile impurities it was dehydrated by applying a low-pressure vacuum of 1 to 10 Pa at temperature T = 423.15 K for 48 h using magnetic stirring. The water content of dried IL was determined using Karl Fischer titration and found to be less than a mass fraction of $3\cdot10^{-4}$.

The density measurements at ambient pressure were also carried out using the Anton-Paar DMA 5000 densimeter with an uncertainty of ±0.01 K. The overall uncertainty of the experimental density measurements at ambient pressure is better than $\Delta\rho = \pm2\cdot10^{-2}$ kg·m^{-3}.

The constant pressure specific heat capacities $c_p(p_0,T)$ were measured at T = (273.15 to 413.15) K using a Pyris 1 DSC Differential Scanning Calorimeter from Perkin Elmer Inc. The obtained experimental data were used for the calculation of the specific heat capacities $c_p(p,T)$ and $c_v(p,T)$ at high pressures and temperatures, in which the density of [BMIM][NTf_2] was experimentally investigated. The accuracy of evaluation of the constant pressure specific heat capacity $c_p(p_0,T)$ was ± 1%.

RESULTS

(p,ρ,T) data of [BMIM][NTf_2] were measured at T = (273.15 to 413.15) K and pressures up to p = 140 MPa and an equation of state (EOS) fitted to the (p,ρ,T) data of [BMIM][NTf_2] is reported. The temperature and pressure steps in the experiments were typically T = (5 to 20) K and p = (5 to 10) MPa, respectively. The constant pressure specific heat capacity $c_p(p_0,T)$ data of [BMIM][NTf_2] were measured at T = (273.15 to 413.15) K. The (p,ρ,T) values obtained are presented in Tables 2 and 3 and the values of constant pressure specific heat capacity $c_p(p_0,T)$ in Table 4.

Table 2: Experimental values of pressure p/MPa, density ρ/kg·m^{-3}, temperature T/K, literature (Harris *et al.*, 2007) and extrapolated viscosity values μ/mPa·s, calculated values of isothermal compressibility $\kappa_T\cdot10^6$/MPa^{-1}, isobaric thermal expansibility $\alpha_p\cdot10^6$/K^{-1}, difference in isobaric and isochoric heat capacities (c_p-c_v)/J·kg^{-1}·K^{-1}, thermal pressure coefficient γ/MPa·K^{-1}, internal pressure p_{int}/MPa, isobaric heat capacity c_p/J·kg^{-1}·K^{-1}, isochoric heat capacity c_v/J·kg^{-1}·K^{-1}, speed of sound u/m·s^{-1} and isentropic expansibility κ_s of 1-butyl-3-methylimidazolium bis(triflluoromethylsulfonyl)imide [BMIM][NTf_2].

p	ρ	T	μ	κ_T	α_p	c_p-c_v	γ	p_{int}	c_p	c_v	U	κ_s
0.101	1460.36	273.15	183.5	484.0	637.7	157.19	1.3176	359.8	1315.33	1158.14	1267.71	23232.90
1.575	1461.35	273.18	187.8	480.5	635.1	156.96	1.3217	359.5	1315.09	1158.13	1271.72	1500.337
4.989	1463.63	273.17	197.8	472.6	629.3	156.42	1.3317	358.8	1314.45	1158.03	1281.08	481.434
10.077	1466.99	273.14	213.0	461.2	621.0	155.67	1.3464	357.7	1313.51	1157.83	1294.86	244.091
19.746	1473.26	273.14	243.5	441.2	606.3	154.44	1.3741	355.6	1311.91	1157.47	1320.39	130.093
29.997	1479.73	273.14	279.0	421.9	592.1	153.34	1.4033	353.3	1310.34	1157.00	1346.71	89.480
39.393	1485.49	273.13	315.6	405.8	580.2	152.50	1.4298	351.1	1308.98	1156.48	1370.18	70.807
49.998	1491.81	273.13	362.7	389.1	567.9	151.73	1.4596	348.7	1307.55	1155.83	1396.01	58.156
59.843	1497.50	273.13	413.2	374.8	557.3	151.15	1.4870	346.3	1306.29	1155.14	1419.39	50.419
69.997	1503.19	273.14	473.1	361.2	547.3	150.69	1.5152	343.9	1305.05	1154.36	1442.96	44.715
79.504	1508.35	273.16	537.5	349.4	538.6	150.37	1.5415	341.6	1303.94	1153.57	1464.57	40.693
90.098	1513.91	273.15	619.9	337.1	529.6	150.10	1.5708	339.0	1302.68	1152.58	1488.14	37.208
99.368	1518.61	273.14	702.1	327.1	522.2	149.95	1.5963	336.7	1301.59	1151.64	1508.39	34.768
109.933	1523.78	273.14	808.4	316.5	514.4	149.87	1.6253	334.0	1300.37	1150.50	1531.01	32.487
120.411	1528.71	273.13	928.4	306.6	507.1	149.87	1.6540	331.4	1299.15	1149.28	1553.05	30.620
129.932	1533.03	273.15	1050.8	298.2	500.9	149.95	1.6800	329.0	1298.09	1148.14	1572.70	29.182
139.613	1537.25	273.16	1189.3	290.1	495.0	150.09	1.7065	326.5	1296.99	1146.90	1592.40	27.923
0.101	1450.91	283.15	105.0	502.0	643.4	160.91	1.2815	362.8	1329.85	1168.94	1249.78	22436.06
1.202	1451.68	283.18	106.7	499.3	641.4	160.73	1.2846	362.6	1329.69	1168.96	1252.85	1895.510
5.187	1454.48	283.15	112.9	489.2	634.2	160.07	1.2965	361.9	1328.94	1168.87	1264.10	448.065
10.200	1457.94	283.16	121.1	477.2	625.7	159.33	1.3111	361.1	1328.12	1168.79	1277.97	233.446
20.191	1464.67	283.16	139.0	455.1	610.0	158.04	1.3403	359.3	1326.58	1168.54	1305.02	123.551
30.101	1471.12	283.16	158.8	435.2	595.8	157.00	1.3691	357.6	1325.21	1168.21	1331.08	86.599
40.081	1477.39	283.16	181.3	416.9	582.9	156.16	1.3980	355.8	1323.95	1167.79	1356.62	67.844
49.997	1483.42	283.15	206.3	400.3	571.1	155.51	1.4266	354.0	1322.78	1167.28	1381.38	56.621

Continuation Table 2

Continuation Table 2

p	ρ	T	μ	κ_T	α_p	c_p-c_v	γ	p_{int}	c_p	c_v	U	κ_s
60.008	1489.30	283.15	234.5	384.9	560.2	155.01	1.4554	352.1	1321.70	1166.69	1405.73	49.045
69.998	1494.97	283.15	266.1	370.8	550.2	154.66	1.4840	350.2	1320.68	1166.03	1429.49	43.643
79.898	1500.41	283.15	300.9	357.7	541.1	154.43	1.5124	348.3	1319.73	1165.29	1452.56	39.622
89.997	1505.76	283.15	340.3	345.5	532.4	154.32	1.5413	346.4	1318.79	1164.47	1475.54	36.426
99.512	1510.65	283.14	381.4	334.7	524.9	154.31	1.5685	344.6	1317.92	1163.61	1496.81	34.010
109.970	1515.84	283.15	431.4	323.6	517.2	154.40	1.5983	342.6	1317.02	1162.61	1519.77	31.837
119.657	1520.51	283.16	482.3	314.0	510.5	154.58	1.6259	340.7	1316.20	1161.63	1540.57	30.158
129.968	1525.31	283.15	541.9	304.4	503.9	154.83	1.6553	338.7	1315.31	1160.47	1562.40	28.650
139.481	1529.61	283.15	602.1	296.1	498.1	155.14	1.6825	336.9	1314.50	1159.36	1582.22	27.456
0.101	1441.48	293.15	63.8	521.0	648.4	164.11	1.2445	364.7	1344.01	1179.90	1231.57	21646.99
1.418	1442.44	293.16	64.8	517.3	645.9	163.87	1.2484	364.6	1343.78	1179.91	1235.40	1552.518
4.886	1444.98	293.15	67.7	507.9	639.3	163.27	1.2588	364.1	1343.16	1179.89	1245.41	458.711
9.795	1448.52	293.15	71.8	495.2	630.5	162.49	1.2734	363.5	1342.35	1179.86	1259.41	234.566
19.754	1455.48	293.16	81.0	471.3	614.1	161.14	1.3028	362.2	1340.87	1179.74	1287.13	122.071
29.998	1462.36	293.15	91.6	449.2	598.9	160.03	1.3331	360.8	1339.52	1179.49	1314.81	84.277
39.408	1468.44	293.15	102.4	430.8	586.2	159.24	1.3608	359.5	1338.42	1179.19	1339.54	66.865
49.997	1475.02	293.15	116.0	411.8	573.2	158.56	1.3919	358.0	1337.32	1178.76	1366.65	55.104
59.813	1480.90	293.15	130.0	395.8	562.3	158.13	1.4207	356.7	1336.40	1178.27	1391.12	47.914
69.996	1486.77	293.15	146.3	380.4	551.9	157.84	1.4506	355.2	1335.52	1177.69	1415.94	42.585
79.504	1492.07	293.15	163.1	367.2	542.9	157.70	1.4784	353.9	1334.77	1177.07	1438.62	38.841
89.996	1497.71	293.15	183.7	353.7	533.8	157.69	1.5092	352.4	1333.99	1176.30	1463.08	35.624
99.217	1502.52	293.15	203.8	342.7	526.4	157.78	1.5362	351.1	1333.34	1175.56	1484.18	33.359
109.936	1507.94	293.15	229.7	330.7	518.5	158.01	1.5677	349.6	1332.63	1174.62	1508.26	31.203
118.950	1512.36	293.15	253.9	321.3	512.3	158.28	1.5941	348.4	1332.05	1173.77	1528.11	29.690
129.935	1517.61	293.15	286.3	310.6	505.2	158.71	1.6264	346.9	1331.37	1172.65	1551.91	28.131
139.274	1521.97	293.15	316.9	302.1	499.6	159.16	1.6540	345.6	1330.80	1171.64	1571.81	26.999
0.101	1436.76	298.15	51.0	530.9	650.8	165.55	1.2259	365.4	1350.99	1185.44	1222.32	21253.85
1.235	1437.63	298.16	51.7	527.6	648.6	165.34	1.2292	365.3	1350.80	1185.46	1225.66	1748.707
5.002	1440.47	298.15	54.1	516.9	641.3	164.66	1.2405	364.9	1350.12	1185.46	1236.73	440.459
10.006	1444.18	298.14	57.4	503.4	632.1	163.83	1.2555	364.3	1349.27	1185.44	1251.21	225.949
19.968	1451.31	298.15	64.7	478.7	615.3	162.45	1.2852	363.2	1347.81	1185.36	1279.29	118.943
29.954	1458.14	298.13	72.8	456.4	600.1	161.34	1.3149	362.0	1346.49	1185.15	1306.65	83.105
39.952	1464.68	298.15	81.7	436.2	586.4	160.50	1.3444	360.9	1345.39	1184.89	1333.21	65.157
50.004	1470.98	298.17	91.7	417.7	573.9	159.88	1.3741	359.7	1344.42	1184.54	1359.20	54.340
59.925	1476.95	298.15	102.6	401.0	562.7	159.45	1.4035	358.5	1343.51	1184.06	1384.29	47.225
69.987	1482.78	298.16	114.8	385.4	552.3	159.19	1.4332	357.3	1342.72	1183.53	1409.09	42.063
79.958	1488.34	298.15	128.1	371.1	542.9	159.08	1.4627	356.1	1341.98	1182.90	1433.13	38.229
90.005	1493.74	298.14	142.8	357.9	534.1	159.11	1.4925	355.0	1341.29	1182.18	1456.86	35.224
99.978	1498.95	298.15	159.0	345.7	526.1	159.26	1.5220	353.8	1340.68	1181.42	1479.92	32.837
109.968	1504.02	298.13	176.8	334.3	518.7	159.52	1.5517	352.6	1340.07	1180.55	1502.60	30.881
119.945	1508.95	298.15	196.5	323.7	511.8	159.89	1.5812	351.5	1339.55	1179.66	1524.80	29.251
129.968	1513.80	298.15	218.3	313.7	505.3	160.35	1.6111	350.4	1339.02	1178.67	1546.75	27.866
139.958	1518.55	298.15	242.3	304.3	499.4	160.89	1.6409	349.3	1338.50	1177.62	1568.28	26.685
0.101	1422.66	313.15	28.6	562.3	657.8	169.39	1.1699	366.3	1371.69	1202.30	1194.22	20089.60
1.418	1423.71	313.11	29.0	557.8	654.9	169.10	1.1741	366.2	1371.38	1202.28	1198.36	1441.978
5.204	1426.67	313.12	30.2	545.8	647.0	168.33	1.1855	366.0	1370.68	1202.35	1209.94	401.377
9.765	1430.17	313.17	31.8	532.0	637.9	167.49	1.1991	365.8	1369.96	1202.46	1223.62	219.301
20.347	1438.02	313.17	35.6	502.6	618.7	165.86	1.2310	365.2	1368.34	1202.48	1254.71	111.270
30.098	1444.93	313.15	39.4	478.4	602.9	164.69	1.2604	364.6	1367.06	1202.37	1282.50	78.967
39.571	1451.36	313.14	43.5	457.1	589.1	163.83	1.2890	364.1	1365.99	1202.17	1308.74	62.825
49.997	1458.16	313.14	48.4	435.9	575.5	163.15	1.3203	363.4	1365.01	1201.85	1336.76	52.117
59.573	1464.14	313.14	53.4	418.1	564.1	162.75	1.3491	362.9	1364.23	1201.48	1361.86	45.584
69.996	1470.41	313.14	59.2	400.5	552.8	162.51	1.3805	362.3	1363.49	1200.97	1388.54	40.503
80.187	1476.30	313.14	65.4	384.7	542.8	162.47	1.4111	361.7	1362.86	1200.39	1413.96	36.809
89.997	1481.76	313.15	72.0	370.6	534.0	162.58	1.4407	361.2	1362.35	1199.77	1437.91	34.043
99.768	1487.03	313.16	79.0	357.7	525.9	162.83	1.4703	360.7	1361.90	1199.07	1461.30	31.829
109.837	1492.30	313.16	86.8	345.3	518.2	163.20	1.5008	360.2	1361.47	1198.27	1484.93	29.959
120.111	1497.53	313.16	95.5	333.5	511.0	163.71	1.5321	359.7	1361.08	1197.37	1508.60	28.376
129.837	1502.36	313.16	104.4	323.1	504.7	164.29	1.5618	359.2	1360.75	1196.46	1530.61	27.108
139.857	1507.23	313.16	114.3	313.1	498.6	164.98	1.5925	358.8	1360.43	1195.45	1552.93	25.988

Continuation Table 2

Continuation Table 2

p	ρ	T	μ	κ_T	α_p	c_p-c_v	γ	p_{int}	c_p	c_v	U	κ_s
0.101	1403.91	333.15	15.4	608.7	667.4	173.66	1.0965	365.2	1398.98	1225.33	1155.86	18572.06
1.571	1405.16	333.12	15.6	602.8	663.8	173.28	1.1012	365.2	1398.62	1225.34	1160.74	1205.209
5.018	1408.08	333.13	16.2	589.8	655.7	172.46	1.1117	365.3	1397.91	1225.45	1171.93	385.414
9.573	1411.84	333.15	16.9	573.5	645.6	171.47	1.1256	365.4	1397.05	1225.58	1186.47	207.619
19.998	1420.12	333.15	18.7	539.5	624.5	169.60	1.1576	365.7	1395.28	1225.68	1218.94	105.511
29.997	1427.65	333.14	20.5	510.6	606.7	168.23	1.1882	365.8	1393.86	1225.63	1249.02	74.244
39.634	1434.56	333.13	22.5	485.7	591.5	167.26	1.2177	366.0	1392.70	1225.44	1277.13	59.032
49.997	1441.63	333.15	24.7	461.7	576.8	166.53	1.2492	366.2	1391.69	1225.16	1306.42	49.208
59.796	1448.01	333.16	26.9	441.1	564.3	166.10	1.2792	366.4	1390.87	1224.77	1333.39	43.050
69.997	1454.35	333.15	29.5	421.7	552.6	165.88	1.3104	366.6	1390.12	1224.23	1360.75	38.470
79.530	1460.04	333.14	32.0	405.0	542.6	165.87	1.3397	366.8	1389.52	1223.64	1385.72	35.251
89.997	1466.07	333.15	34.9	388.3	532.7	166.05	1.3718	367.0	1388.98	1222.93	1412.49	32.501
99.488	1471.34	333.15	37.8	374.3	524.4	166.36	1.4011	367.3	1388.55	1222.19	1436.29	30.510
109.844	1476.92	333.15	41.0	360.2	516.2	166.84	1.4330	367.6	1388.16	1221.31	1461.66	28.727
119.474	1481.98	333.15	44.3	348.0	509.1	167.42	1.4629	367.9	1387.85	1220.43	1484.83	27.349
129.847	1487.32	333.14	47.9	335.8	502.1	168.16	1.4952	368.3	1387.55	1219.39	1509.36	26.095
139.470	1492.20	333.13	51.5	325.3	496.1	168.95	1.5252	368.6	1387.31	1218.36	1531.69	25.099
0.101	1385.21	353.15	9.6	660.8	677.5	177.09	1.0253	362.0	1426.08	1248.98	1116.88	17108.91
2.062	1386.99	353.16	9.7	651.7	672.2	176.54	1.0315	362.2	1425.62	1249.08	1123.71	849.380
4.981	1389.60	353.16	10.0	638.6	664.6	175.76	1.0407	362.6	1424.94	1249.18	1133.79	358.632
9.972	1393.97	353.15	10.4	617.4	652.3	174.57	1.0565	363.1	1423.86	1249.30	1150.76	185.120
19.715	1402.15	353.16	11.3	580.1	630.6	172.65	1.0870	364.2	1422.05	1249.41	1182.88	99.513
29.997	1410.34	353.15	12.3	545.6	610.6	171.12	1.1192	365.2	1420.43	1249.30	1215.59	69.472
39.906	1417.81	353.14	13.4	516.2	593.7	170.07	1.1501	366.2	1419.10	1249.03	1246.02	55.158
49.994	1425.04	353.15	14.5	489.5	578.3	169.34	1.1815	367.3	1417.96	1248.62	1276.02	46.408
60.299	1432.06	353.16	15.7	465.0	564.3	168.91	1.2136	368.3	1416.98	1248.07	1305.76	40.490
69.997	1438.36	353.16	17.0	444.2	552.5	168.74	1.2438	369.3	1416.16	1247.42	1333.02	36.512
79.453	1444.25	353.16	18.2	425.7	542.1	168.78	1.2733	370.2	1415.47	1246.69	1358.92	33.566
89.995	1450.53	353.15	19.7	406.9	531.5	169.03	1.3062	371.3	1414.78	1245.76	1387.13	31.014
99.161	1455.81	353.13	21.1	391.9	523.1	169.39	1.3350	372.3	1414.25	1244.85	1411.14	29.237
109.841	1461.76	353.15	22.8	375.8	514.2	169.99	1.3684	373.4	1413.75	1243.76	1438.48	27.539
120.136	1467.33	353.17	24.4	361.5	506.4	170.71	1.4007	374.5	1413.34	1242.63	1464.24	26.188
129.833	1472.46	353.17	26.1	349.1	499.6	171.50	1.4313	375.6	1412.98	1241.48	1488.08	25.114
139.753	1477.61	353.17	27.8	337.2	493.2	172.42	1.4626	376.8	1412.66	1240.23	1512.04	24.171
0.101	1366.59	373.15	6.6	718.6	687.2	179.46	0.9563	356.7	1452.72	1273.26	1077.91	15719.82
1.253	1367.68	373.14	6.6	712.1	683.7	179.12	0.9601	357.0	1452.42	1273.31	1082.22	1278.335
4.940	1371.17	373.13	6.8	692.3	673.1	178.10	0.9723	357.9	1451.53	1273.43	1095.82	333.301
10.088	1375.93	373.15	7.1	666.5	659.3	176.84	0.9891	359.0	1450.43	1273.58	1114.35	169.371
20.181	1384.85	373.16	7.7	621.4	635.1	174.88	1.0220	361.2	1448.49	1273.61	1149.56	90.687
29.994	1393.07	373.15	8.3	583.3	614.6	173.49	1.0538	363.2	1446.86	1273.36	1182.52	64.949
39.415	1400.57	373.15	8.9	551.1	597.4	172.56	1.0841	365.1	1445.50	1272.94	1212.98	52.282
49.994	1408.55	373.16	9.6	519.0	580.3	171.90	1.1181	367.2	1444.18	1272.28	1246.07	43.745
60.032	1415.74	373.17	10.3	492.0	566.0	171.60	1.1502	369.2	1443.07	1271.47	1276.47	38.424
69.993	1422.52	373.15	11.0	467.9	553.2	171.56	1.1822	371.1	1442.05	1270.50	1305.83	34.655
79.488	1428.69	373.13	11.8	447.2	542.2	171.72	1.2126	373.0	1441.17	1269.45	1333.03	31.938
89.995	1435.23	373.15	12.6	426.4	531.3	172.12	1.2461	375.0	1440.34	1268.22	1362.35	29.599
99.429	1440.87	373.16	13.4	409.3	522.3	172.64	1.2762	376.8	1439.65	1267.01	1388.06	27.921
109.846	1446.85	373.16	14.3	392.0	513.3	173.36	1.3095	378.8	1438.93	1265.57	1415.85	26.405
120.742	1452.90	373.17	15.3	375.5	504.8	174.28	1.3443	380.9	1438.26	1263.98	1444.22	25.099
129.844	1457.80	373.17	16.1	362.7	498.2	175.16	1.3735	382.7	1437.73	1262.58	1467.47	24.179
139.897	1463.09	373.17	17.0	349.6	491.5	176.23	1.4058	384.7	1437.19	1260.96	1492.68	23.302
0.101	1348.03	393.15	4.9	781.5	694.6	180.12	0.8889	349.4	1478.29	1298.17	1039.82	14427.42
2.049	1349.98	393.14	5.0	768.6	688.4	179.61	0.8957	350.1	1477.86	1298.25	1047.54	722.863
5.204	1353.10	393.14	5.1	748.6	678.8	178.85	0.9068	351.3	1477.20	1298.36	1059.86	292.047
10.321	1358.04	393.14	5.3	718.5	664.3	177.78	0.9245	353.1	1476.21	1298.43	1079.43	153.317
20.391	1367.39	393.16	5.7	666.1	638.9	176.17	0.9591	356.7	1474.48	1298.31	1116.54	83.609
29.995	1375.85	393.15	6.0	623.1	618.1	175.15	0.9919	360.0	1472.98	1297.84	1150.51	60.724
39.559	1383.86	393.15	6.4	585.7	599.9	174.53	1.0242	363.1	1471.64	1297.11	1183.06	48.968
49.993	1392.15	393.15	6.9	549.9	582.5	174.23	1.0593	366.5	1470.31	1296.08	1217.31	41.267
60.279	1399.89	393.15	7.4	518.7	567.3	174.25	1.0936	369.7	1469.08	1294.83	1249.94	36.284

Continuation Table 2

Continuation Table 2

p	ρ	T	μ	κ_T	α_p	c_p-c_v	γ	p_{int}	c_p	c_v	U	κ_s
69.992	1406.84	393.15	7.8	492.6	554.6	174.51	1.1259	372.7	1468.00	1293.49	1279.77	32.919
80.121	1413.73	393.16	8.3	468.0	542.7	174.99	1.1595	375.7	1466.94	1291.95	1310.01	30.279
89.994	1420.13	393.16	8.8	446.4	532.2	175.65	1.1921	378.7	1465.95	1290.31	1338.72	28.279
99.459	1426.01	393.16	9.3	427.6	523.0	176.42	1.2233	381.5	1465.04	1288.62	1365.58	26.735
109.834	1432.16	393.16	9.8	408.7	513.9	177.41	1.2575	384.6	1464.08	1286.67	1394.36	25.351
119.422	1437.62	393.16	10.4	392.7	506.2	178.44	1.2890	387.4	1463.23	1284.79	1420.31	24.284
129.833	1443.32	393.16	11.0	376.8	498.5	179.67	1.3232	390.4	1462.34	1282.67	1447.93	23.307
139.501	1448.43	393.16	11.6	363.1	491.9	180.91	1.3549	393.2	1461.54	1280.63	1473.07	22.532
0.101	1329.54	413.15	3.8	847.4	696.9	178.18	0.8224	339.7	1501.90	1323.72	1003.70	13256.64
1.024	1330.50	413.13	3.8	840.1	693.9	178.02	0.8260	340.2	1501.76	1323.73	1007.62	1318.836
5.002	1334.61	413.15	3.9	810.3	681.4	177.40	0.8409	342.4	1501.28	1323.88	1024.08	279.791
10.410	1340.07	413.16	4.1	773.1	665.7	176.73	0.8611	345.4	1500.63	1323.90	1045.95	140.843
20.251	1349.64	413.16	4.4	713.8	640.7	175.96	0.8975	350.5	1499.48	1323.52	1084.26	78.372
29.996	1358.66	413.16	4.7	663.9	619.4	175.66	0.9330	355.5	1498.38	1322.72	1120.50	56.887
40.087	1367.55	413.16	5.0	619.3	600.2	175.73	0.9693	360.4	1497.26	1321.53	1156.49	45.640
49.992	1375.83	413.15	5.3	581.2	583.8	176.09	1.0046	365.1	1496.14	1320.05	1190.47	39.011
60.368	1384.07	413.15	5.6	546.2	568.7	176.74	1.0412	369.8	1494.99	1318.24	1224.81	34.397
69.992	1391.31	413.15	5.9	517.4	556.2	177.54	1.0750	374.1	1493.91	1316.36	1255.63	31.339
80.288	1398.68	413.14	6.3	489.9	544.2	178.57	1.1108	378.6	1492.73	1314.15	1287.64	28.880
89.996	1405.26	413.14	6.6	466.6	534.0	179.69	1.1445	382.8	1491.63	1311.93	1316.98	27.078
99.338	1411.29	413.14	6.9	446.2	525.0	180.88	1.1766	386.8	1490.56	1309.68	1344.48	25.676
109.856	1417.73	413.14	7.3	425.4	515.9	182.33	1.2127	391.2	1489.36	1307.02	1374.71	24.385
120.053	1423.65	413.13	7.7	407.0	507.7	183.84	1.2475	395.3	1488.17	1304.34	1403.32	23.351
129.854	1429.05	413.14	8.0	390.8	500.6	185.37	1.2809	399.3	1487.06	1301.69	1430.21	22.511
139.825	1434.28	413.15	8.4	375.6	493.9	187.00	1.3147	403.4	1485.93	1298.93	1457.01	21.780

Table 3: Experimental density values of [BMIM][NTf$_2$] at p=0.101 MPa measured in an Anton-Paar DMA 5000M vibrating tube densimeter (<353.15 K) and extrapolated using Eqs. (2) - (3) (>353.15 K).

T/K	ρ/kg·m^{-3}
273.15	1460.36
283.15	1450.91
293.15	1441.48
298.15	1436.76
313.15	1422.66
333.15	1403.91
353.15	1385.21
373.15	1366.59
393.15	1348.03
413.15	1329.54

Table 4: Experimental values of specific heat capacity $c_p(p_0,T)$ of [BMIM][NTf$_2$] at p=0.101 MPa and temperatures at T=(273.15 to 413.15) K measured using the Pyris 1 DSC.

T/K	$c_p(p_0,T)$/J·kg^{-1}·K^{-1}
273.15	1315.22
283.15	1329.65
293.15	1343.92
298.15	1351.00
313.15	1371.97
333.15	1399.37
353.15	1426.11
373.15	1452.20
393.15	1477.64
413.15	1502.42

The measured densities as a function of pressure and temperature are fitted to the equation of state (Safarov *et al.*, 2009):

$$p(\rho,T)/\text{MPa} = A(T)\cdot(\rho/\text{g}\cdot\text{cm}^{-3})^2 + B(T)\cdot(\rho/\text{g}\cdot\text{cm}^{-3})^8 + C(T)\cdot(\rho/\text{g}\cdot\text{cm}^{-3})^{12} \quad (2)$$

where: the coefficients of Eq. (2) $A(T)$, $B(T)$ and $C(T)$ are functions of temperature.

$$A(T) = \sum_{i=1}^{4} a_i T^i,\ B(T) = \sum_{i=0}^{3} b_i T^i,\ C(T) = \sum_{i=0}^{3} c_i T^i. \quad (3)$$

The coefficients a_i, b_i and c_i of Eq. (3) are given in Table 5. Eqs. (2) and (3) describe the experimental results of density of [BMIM][NTf$_2$] within $\pm\Delta\rho/\rho$ = ±0.0062% percent, corresponding to $\Delta\rho$ = ± 0.10 kg m^{-3} standard with a maximal deviation of $\Delta\rho$ = ±0.47 kg m^{-3}, respectively.

Figures 1 and 2 show the plots of pressure p of [BMIM][NTf$_2$] versus density ρ and deviations of the experimental density ρ of [BMIM][NTf$_2$] from the calculated density ρ by Eqs. (2) and (3) versus pressure p at T = (273.15 to 413.15) K.

Table 5: Values of the coefficients a_i, b_i and c_i in Eqs. (2) - (3).

a_i	b_i	c_i
$a_1 = -2.52296606$	$b_0 = -47.5329551$	$c_0 = 7.84979326$
$a_2 = 1.11071177 \cdot 10^{-2}$	$b_1 = 0.59043$	$c_1 = -7.50919 \cdot 10^{-2}$
$a_3 = -0.16614126 \cdot 10^{-4}$	$b_2 = -0.18066 \cdot 10^{-2}$	$c_2 = 0.2296674 \cdot 10^{-3}$
$a_4 = 0.75112 \cdot 10^{-8}$	$b_3 = 0.1797 \cdot 10^{-5}$	$c_3 = -0.2124491374 \cdot 10^{-6}$

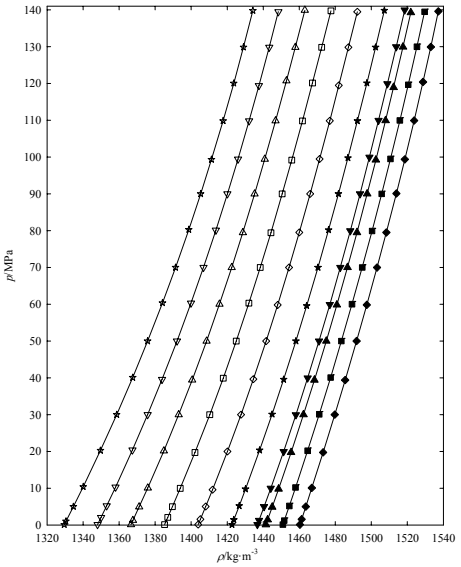

Figure 1: Plot of pressure p of [BMIM][NTf_2] *versus* density ρ: ◆, 273.15 K; ■, 283.15 K; ▲, 293.15 K; ▼, 298.15 K; ★, 313.15 K; ◇, 333.14 K; □, 353.16 K; △, 373.15 K; ▽, 393.15 K; ☆, 413.15 K; _ calculated by Eqs. (2) - (3).

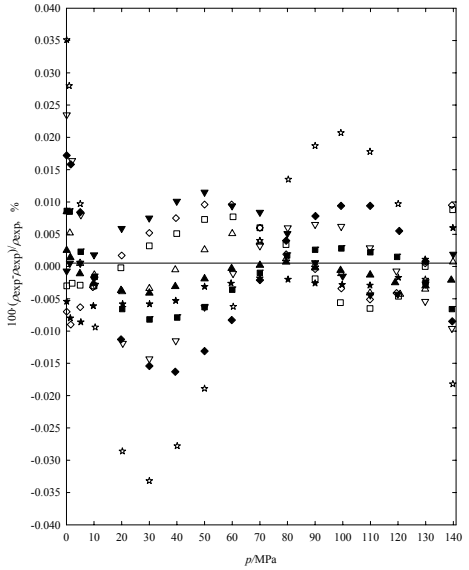

Figure 2: Plot of deviations of experimental density $\rho_{exp.}$ of [BMIM][NTf_2] from that calculated by Eqs. (2) - (3) $\rho_{cal.}$ *versus* pressure p at T=(273.15 to 413.15) K: ◆, 273.15 K; ■, 283.15 K; ▲, 293.15 K; ▼, 298.15 K; ★, 313.15 K; ◇, 333.14 K; □, 353.16 K; △, 373.15 K; ▽, 393.15 K; ☆, 413.15 K.

The values of isothermal compressibility κ_T/MPa^{-1}, isobaric thermal expansibility α_p/K^{-1}, difference in isobaric and isochoric heat capacities (c_p-c_v)/J·kg^{-1}·K^{-1}, thermal pressure coefficient γ/MPa·K^{-1}, internal pressure p_{int}/MPa, isobaric heat capacity c_p/J·kg^{-1}·K^{-1}, isochoric heat capacity c_v/J·kg^{-1}·K^{-1}, speed of sound u/m·s^{-1} and isentropic expansibility κ_s of 1-butyl-3-methylimidazolium bis(triflluoromethylsulfonyl)imide [BMIM][NTf_2] were calculated from Eqs. (2) and (3) using the following fundamental equations of thermodynamics:

- Isothermal compressibility $\kappa_T(p,T)$:

$$\kappa_T(p,T) = \frac{1}{\rho}\left(\frac{\partial p(T,\rho)}{\partial \rho}\right)_T^{-1} \tag{4}$$

$$\kappa_T(p,T) = 1/[2A(T)\rho^2 + 8B(T)\rho^8 + 12C(T)\rho^{12}]. \tag{5}$$

- Isobaric thermal expansibility $\alpha_p(p,T)$:

$$\alpha_p(p,T) = \frac{1}{\rho}\left(\frac{\partial p(T,\rho)}{\partial T}\right)_\rho \left(\frac{\partial p(T,\rho)}{\partial \rho}\right)_T^{-1}. \tag{6}$$

$$\alpha_p(p,T) = [A'(T) + B'(T)\rho^6 + C'(T)\rho^{10}]/ [2A(T) + 8B(T)\rho^6 + 12C(T)\rho^{10}], \tag{7}$$

where: A', B', and C' are the derivatives of A, B, and C, respectively:

$$A'(T) = \sum_{i=1}^{4} i a_i T^{i-1},\ B'(T) = \sum_{i=1}^{3} i b_i T^{i-1},$$
$$C'(T) = \sum_{i=1}^{3} i c_i T^{i-1}. \tag{8}$$

- Thermal pressure coefficient $\gamma(p,T)$:

$$\gamma(p,T) = \frac{\alpha_p(p,T)}{\kappa_T(p,T)}. \tag{9}$$

- Internal pressure $p_{int}(p,T)$:

$$p_{int}(p,T) \equiv \left(\frac{\partial U}{\partial V}\right)_T = T\left(\frac{\partial p(T,\rho)}{\partial T}\right)_V - p$$
$$= T \cdot \gamma(p,T) - p = \frac{T \cdot \alpha_p(p,T)}{\kappa_T(p,T)} - p \tag{10}$$

▪ Specific heat capacities (at constant pressure $c_p(p,T)$/J·kg^{-1}·K^{-1} and constant volume $c_v(p,T)$/J·kg^{-1}·K^{-1}) at high pressures and temperatures:

$$c_v(p,T) = c_v(p_0,T) - T\int_{\rho_0}^{\rho}\left(\frac{\partial^2 p(T,\rho)}{\partial T^2}\right)_\rho \frac{d\rho}{\rho^2}, \quad (11)$$

$$c_p(p,T) = c_v(p,T) + \frac{T\left(\frac{\partial p(T,\rho)}{\partial T}\right)_\rho^2}{\rho^2\left(\frac{\partial p(T,\rho)}{\partial \rho}\right)_T}, \quad (12)$$

$$c_p(p,T) - c_v(p,T) = \frac{\alpha_p^2(p,T)\cdot T}{\rho\cdot\kappa_T(p,T)}. \quad (13)$$

After determination of specific heat capacities it is possible to determine the speed of sound at high pressures and various temperatures $u(p,T)$/m·s^{-1} using the following thermodynamic relation:

$$u^2(p,T) = \frac{c_p(p,T)}{c_v(p,T)}\left(\frac{\partial p(T,\rho)}{\partial \rho}\right)_T. \quad (14)$$

We can also obtain the isentropic expansion $\kappa_s(p,T)$ using the following relation:

$$\kappa_s(p,T) = \frac{\rho(p,T)}{p}\cdot\frac{c_p(p,T)}{c_v(p,T)}\cdot\left(\frac{\partial p(T,\rho)}{\partial \rho}\right)_T. \quad (15)$$

These values are also presented in Table 2 together with (p,ρ,T) data of [BMIM][NTf$_2$].

If we can define the constant volume specific heat capacity at ambient pressure $c_v(p_0,T)$ in Eq. (11), it is possible to calculate the specific heat capacities at high pressures and temperatures [$c_v(p,T)$ in Eq. (11) and $c_p(p,T)$ in Eq. (12)], in which the density of [BMIM][NTf$_2$] is experimentally investigated. The second term on the right side of Eq. (12) is the differences in specific heat capacities $c_p(p,T)$ – $c_v(p,T)$/J·kg^{-1}·K^{-1}, which were calculated using the (p,ρ,T) values. The constant volume specific heat capacities at ambient pressure $c_v(p_0,T)$ were calculated using the experimental constant pressure specific heat capacity $c_p(p_0,T)$ values at ambient pressure and Eq. (13) for the ambient pressure situation.

DISCUSSION

The measured (p,ρ,T) data of [BMIM][NTf$_2$] and calculated thermophysical properties are analyzed and compared with the available literature values (Table 1),. The percent (PD) and average relative deviations (APD) between the literature values and our experimental density values are calculated using Eqs. (16) - (17) from Safarov *et al.* (2013). The equation of state was used to interpolate our results with the literature values at similar temperature and pressure conditions for comparison purposes. Figure 3 show the plot of deviation of experimental $\rho_{exp.}$ and literature $\rho_{cal.}$ densities of [BMIM][NTf$_2$] at p=0.101 MPa *versus* temperature, which are discussed below.

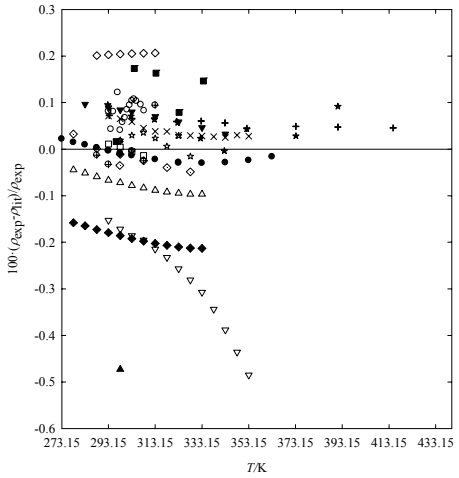

Figure 3: Plot of deviation of experimental $\rho_{exp.}$ and literature $\rho_{cal.}$ densities of [BMIM][NTf$_2$] at p=0.101 MPa *versus* temperature: ▲, Huddleston *et al.* (2001); x, Krummen *et al.* (2002); ■, Fredlake *et al.* (2004); ◇, Tokuda *et al.* (2005); ☆, de Azevedo *et al.* (2005); ★, Jacquemin *et al.* (2006); ⊕, Tokuda *et al.* (2006); ◆, Troncoso *et al.* (QUILL sample) (2006); △, Troncoso *et al.* (Covalent Associates sample) (2006); +, Jacquemin *et al.* (2007); ●, Harris *et al.* (2007); ○, Katsuta *et al.* (2010); □, Geppert-Rybczyńska *et al.* (2010); ▽,Vranes *et al.* (2012).

The earliest density value of IL in the literature obtained by Huddleston *et al.* (2001) at T = 298.15 K has $\Delta\rho/\rho$ = 0.4729% deviation with our value. This large deviation was due to the gravimetric analysis using a pycnometer in the study.

The next thirteen measured density values in the wide range of temperature T = (293.15 to 353.15) K at ambient pressure, published by Krummen *et al.*, (2002) were also compared with our values. The average deviation of these is $\Delta\rho/\rho$ = ± 0.0395%. These literature values are slightly higher than our values.

The average deviation of five density values of Fredlake *et al.* (2004) from our values is $\Delta\rho/\rho$ = ±0.1156%. These literature values are higher than our values due to the fact that the observed deviation was a result of gravimetric analysis using a pycnometer in the study similar to Huddleston *et al.* (2001). The maximum deviation of these values is $\Delta\rho/\rho$ = 0.1732% at T = 304.15 K.

The six density results for IL of Tokuda *et al.* (2005) are also higher than our values, with an average deviation of $\Delta\rho/\rho$ = ±0.2042%.

Azevedo *et al.* (2005) provided the seven density results of [BMIM][NTF_2], which have $\Delta\rho/\rho$ = 0.0226% average deviation from our measured results. These values are higher than ours, except the last value at T = 328.15 K. The maximum deviation is $\Delta\rho/\rho$ = ±0.0356% at T = 308.09 K.

The nine values of Jacquemin *et al.* (2006) have $\Delta\rho/\rho$ = ±0.0530% average deviation from our results and these values are higher than ours, except the value at T = 342.72 K. The maximum deviation of this comparison is $\Delta\rho/\rho$ = 0.0951% at T = 292.88 K.

The other six values of Tokuda *et al.* (2006) have $\Delta\rho/\rho$ = ±0.0309% average deviation with our experimental values. The values are mostly smaller than our density results. The maximum uncertainty of results is $\Delta\rho/\rho$ = -0.0943% at T = 313.15 K.

The twelve density results of the QUILL sample [BMIM][NTF_2] used by Troncoso *et al.* (2006) have $\Delta\rho/\rho$ = ±0.1913% average deviation and they are smaller than our values. The comparison of the other [BMIM][NTF_2] sample from Covalent Associates also used used by Troncoso *et al.*, (2006) showed $\Delta\rho/\rho$ = 0.0769% average deviation and they are also smaller than our values with a maximum deviation of $\Delta\rho/\rho$ = -0.0966% at T = 333.15 K.

Jacquemin *et al.* (2007) presented ten density values at ambient pressure and various temperatures, which have $\Delta\rho/\rho$ = ±0.0516% average deviation and these values are higher than our measured values. The maximum deviation is $\Delta\rho/\rho$ = 0.0726% at T = 293.49 K.

The sixteen values of Harris *et al.* (2007) have $\Delta\rho/\rho$ = ±0.0168% average deviation with our values. These literature results are in good agreement with our values at the all measured temperatures. The maximum deviation is $\Delta\rho/\rho$ = 0.0303% at T = 333.15 K.

The comparison of fourteen density results of Katsuta *et al.* (2010) with our results showed $\Delta\rho/\rho$ = ±0.0830% average deviation. These values are mostly higher than our values with a maximum deviation of $\Delta\rho/\rho$ = 0.1215% at T = 297.10 K.

The four density results of Geppert-Rybczyńska *et al.* (2010) are compared with our density results and an average deviation of $\Delta\rho/\rho$ = ±0.0087% is obtained.

The thirteen density values of Vranes *et al.* (2012) have $\Delta\rho/\rho$ = ±0.2809% average deviation with our experimental values. These values are smaller than our results with a minimal $\Delta\rho/\rho$ = -0.4850% deviation at T = 353.15 K.

There are two (p,ρ,T) literature investigations (Azevedo *et al.*, 2005; Jacquemin *et al.*, 2007) of [BMIM][NTf_2]:

- The 168 density values of de Azevedo *et al.* (2005) are mostly smaller than our values with an $\Delta\rho/\rho$ = ±0.0507% average deviation. The minimum deviation of these literature values is $\Delta\rho/\rho$ = -0.1182% at T = 328.20 K and p = 46.80 MPa (Figure 9).
- The 36 density results of Jacquemin *et al.* (2007) at high pressures and various temperatures are compared with our results. These results have positive and negative deviation from our results (Figure 4) with a $\Delta\rho/\rho$ = ±0.0325% average deviation. The maximum deviation of these at T = 414.92 K and p = 1 MPa is $\Delta\rho/\rho$ = 0.079%.

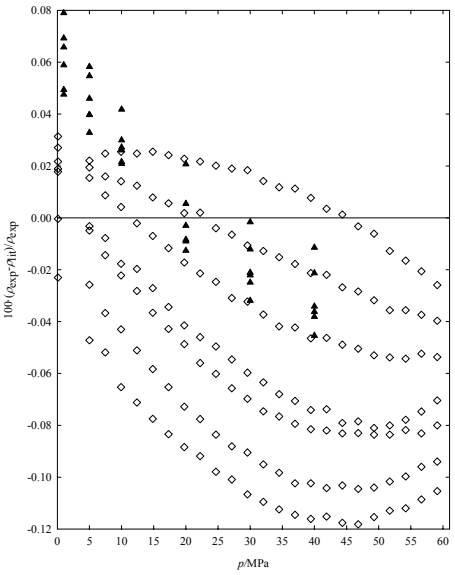

Figure 4: Plot of deviation of experimental $\rho_{exp.}$ and literature $\rho_{cal.}$ densities of [BMIM][NTf_2] at various temperatures *versus* pressure p/MPa: ◇, de Azevedo *et al.*, (2005); ▲, Jacquemin *et al.*, (2007).

Various heat capacity values at constant ambient pressure $c_p(p_0,T)$ are available in the literature (Krummen *et al.*, 2002; Fredlake *et al.*, 2004; Tokuda *et al.*, 2006; Troncoso *et al.*, 2006; Shimizu *et al.*, 2007; Ge *et al.*, 2008; Blokhin *et al.*, 2008; Katsuta *et al.*, 2010). Our results are in good agreement with the values from Tokuda *et al.* (2006),

Shimizu *et al.* (2007) and Ge *et al.* (2008). The deviations from the literature values are presented in Figure 5.

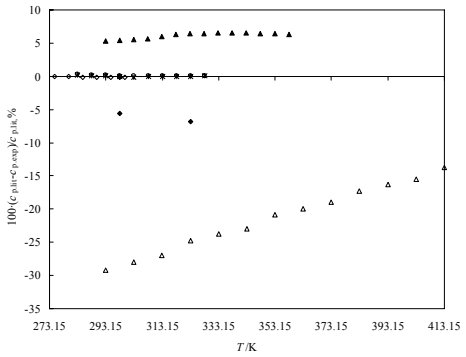

Figure 5: Plot of deviation of literature heat capacities $c_p(p_0,T)$/J·kg^{-1}·K^{-1} values of [BMIM][NTf$_2$] at constant ambient pressure from our measured values *versus* temperature: ▲, Ge *et al.* (2008); ■, Blokhin *et al.* (2008); ◆, Fredlake *et al.* (2004); △, Holbrey *et al.* (2003); ◇, Shimizu *et al.* (2007); ○, Troncoso (QUILL) (2006); *, Troncoso (Covalent Associates) (2006).

The 10 heat capacity values at constant ambient pressure $c_p(p_0,T)$ of the QUILL sample [BMIM][NTF$_2$] used by Troncoso *et al.* (2006) have $\Delta c_p/c_p$ = 0.13% average deviation and they are higher than our values. The comparison of the other 10 heat capacity values at constant ambient pressure $c_p(p_0,T)$ for the [BMIM][NTF$_2$] sample from Covalent Associates also used by Troncoso *et al.* (2006) showed $\Delta c_p/c_p$ = ±0.08% average deviation. These values are higher than our values at lower temperatures and, after T = 298.15 K, the literature values are smaller than our values. The maximum deviation of this comparison is $\Delta c_p/c_p$ = 0.36% at T = 283.15 K for the QUILL sample.

The 12 heat capacity values at constant ambient pressure $c_p(p_0,T)$ presented by Shimizu *et al.* (2007) have $\Delta c_p/c_p$ = ±0.18% average deviation from our results. We used all the literature values at the temperatures T = (250 to 300) K for the comparison. These values are higher than our values at lower temperatures and, after T = 280 K, the literature values are smaller than our values. These experimental values show good agreement with our extrapolated values for all of the temperature intervals and the maximum deviation of this comparison is $\Delta c_p/c_p$ = 0.46% at T = 250 K.

The experimental values of Blokhin *et al.* (2008) after T = 190 K were compared to our extrapolated values and the result of this comparison shows good agreement with an average deviation of $\Delta c_p/c_p$ = 1.34%.

The thirty eight high pressure speed of sound values of de Azevedo *et al.* (2005) were compared with our results. The average deviation of these comparison was $\Delta u/u$ = ±0.9808%. The maximum deviation of these literature values is $\Delta u/u$ = 2.3129% at T = 283.15 K and p = 79.70 MPa.

The internal pressure decreases with increasing pressure for the temperatures between 273.15 to 313.15 K, and increases for the temperatures above 333.15 K. This interesting behaviour can be explained by the resultant forces under low-pressure conditions that are attractive and, as the pressure increases, the repulsive forces become dominant at low temperatures for the IL. It is also observed that p_{int} increases with respect to temperature at fixed pressure for p > 60 MPa for the IL. On the other hand, the internal pressure decreases with increase in temperature for normal liquids due to the fact that the increase in temperature only affects the coordination number, while the intermolecular distances within the liquid molecules remain unchanged (Fedorov and Stashulenok, 1981). This behavior might be related to the self-associated structure of the IL of the cationic part, or inherent structural heterogeneities of the polar and non-polar groups of the IL (Lopes and Padua, 2006).

CONCLUSION

The main objective of the present work is to report (p,ρ,T) measurements of 1-butyl-3-methylimidazolium bis(triflluoromethylsulfonyl)imide [BMIM][NTf$_2$] at T = (273.15 to 413.15) K and pressures up to p = 140 MPa. The constructed empirical equation of state can be used to calculate various thermal and caloric parameters.

All density values from the literature have been compared with our results and show good agreement.

NOMENCLATURE

Symbols

p	Absolute pressure
T	Absolute temperature
c_p	Isobaric heat capacity
c_v	Isochoric heat capacity
u	speed of sound
p_{int}	Internal pressure

U	Internal energy
V	Volume
APD	Average Percent Deviations

Greek Letters

ρ	Density
η	Viscosity
κ_T	Isothermal compressibility
α_p	Isobaric thermal expansibility
γ	Thermal pressure coefficient

REFERENCES

Aschcroft, S. J., Booker, D. R., Turner, J. C. R., Density measurements by oscillating tube. Journal of the Chemical Society, Faraday Transactions, 86, 145-149 (1990).

Bagno, A., Butts, C., Chiappe, C., D'Amico, F., Lord, J. C. D., Pieraccini, D., Rastrelli, F., The effect of the anion on the physical properties of trihalide-based N,N-dialkylimidazolium ionic liquids. Organic & Biomolecular Chemistry, 3, 1624-1630 (2005).

Blokhin, A., Paulechka, Y., Strechan, A., Kabo, G., Physicochemical properties, structure, and conformations of 1-butyl-3-methylimidazolium bis(trifluoromethanesulfonyl)imide $[C_4mim]NTf_2$ ionic liquid. Journal of Physical Chemistry B, 112, 4357-4364 (2008).

de Azevedo, R. G., Esperança, J. M. S. S., Szydlowski, J., Visak, Z. P., Pires, P. F., Guedes, H. J. R., Rebelo, L. P. N., Thermophysical and thermodynamic properties of ionic liquids over an extended pressure range: [bmim][NTf_2] and [hmim][NTf_2]. The Journal of Chemical Thermodynamics, 37, 888-899 (2005).

Dupont, J., On the solid, liquid and solution structural organization of imidazolium ionic liquids. Journal of Brazilian Chemical Society, 15(3), 341-350 (2004).

Fedorov, M. K. and Stashulenok, V. K., Internal pressure and its application for the analysis of the structure of aqueous electrolyte solutions at high temperatures and pressures. Journal of Structure Chemistry, 22, 140-142 (1981).

Fitzgerald, H. and Fitzgerald, D., As assessment of laboratory density meters. Petroleum Review, 544-549 (1992).

Fredlake, C. P., Crosthwaite, J. M., Hert, D. G., Aki, S. N. V. K., Brennecke, J. F., Thermophysical properties of imidazolium-based ionic liquids. Journal of Chemical & Engineering Data, 49, 954-964 (2004).

Ge, R., Hardacre, Ch., Jacquemin, J., Nancarrow, P., Rooney, D. W., Heat capacities of ionic liquids as a function of temperature at 0.1 MPa. Measurement and Prediction, Journal of Chemical & Engineering Data, 53, 2148-2153 (2008).

Geppert-Rybczyńska, M., Heintz, A., Lehmann, J. K., Golus. A., Volumetric properties of binary mixtures containing ionic liquids and some aprotic solvents. Journal of Chemical & Engineering Data, 55, 4114-4120 (2010).

Guliyev, T., Safarov, J., Shahverdiyev, A., Hassel, E., (p,ρ,T) properties and apparent molar volumes V_ϕ of $ZnBr_2$+C_2H_5OH. The Journal of Chemical Thermodynamics, 41, 1162-1169 (2009).

Handy, Scott T., (Ed.) Applications of Ionic Liquids in Science and Technology. InTech (2011).

Harris, K. R., Kanakubo, M., Woolf, L. A., Temperature and pressure dependence of the viscosity of the ionic liquids 1-hexyl-3-methylimidazolium hexafluorophosphate and 1-butyl-3-methylimidazolium bis(trifluoromethylsulfonyl)imide. Journal of Chemical & Engineering Data, 52, 1080-1085 (2007).

Holbrey, J. D., Reichert, W. M., Reddy, R. G., Rogers, R. D., In: Ionic liquids as green solvents: Progress and prospects. ACS Symposium Series, Vol. 856, Edited by R. D. Rogers and K. R. Seddon, American Chemical Society, New York, 121 (2003).

Huddleston, J. G., Visser, A. E., Reichert, W. M., Willauer, H. D., Broker, G. A., Rogers, R. D., Characterization and comparison of hydrophilic and hydrophobic room temperature ionic liquids incorporating the imidazolium cation. Green Chemistry, 3, 156-164 (2001).

Jacquemin, J., Husson, P., Padua, A. A. H., Majer, V., Density and viscosity of several pure and water-saturated ionic liquids. Green Chemistry, 8, 172-180 (2006).

Jacquemin, J., Husson, P., Mayer, V., Cibulka, I., High-pressure volumetric properties of imidazolium-based ionic liquids: Effect of the anion. Journal of Chemical & Engineering Data, 52, 2204-2211 (2007).

Katsuta, S., Shiozawa, Y., Imai, K., Kudo, Y., Takeda, Y., Stability of ion pairs of bis(trifluoromethanesulfonyl)amide-based ionic liquids in dichloromethane. Journal of Chemical & Engineering Data, 55, 1588-1593 (2010).

Kim, K.-I., Shin, B.-K., Ziegler, F., Ionic liquids as new working fluids for use in absorption heat pumps or chillers: Their thermodynamic properties. Abstracts of XV International Symposium of

Thermophysical Properties, Colorado, USA, p. 292 (2003).

Krummen, M., Wasserscheid, P., Gmehling, J., Measurement of activity coefficients at infinite dilution in ionic liquids using the dilutor technique. Journal of Chemical & Engineering Data, 47, 1411-1417 (2002).

Nabiyev, N., Bashirov, M., Safarov, J., Shahverdiyev, A., Hassel, E., Thermodynamic properties of the geothermal resources (Khachmaz and Sabir-oba) of Azerbaijan. Journal of Chemical & Engineering Data, 54, 1799-1806 (2009).

Lopes, J. N. A. C., Padua, A. A. H., Nanostructural organization in ionic liquids. Journal of Physical Chemistry B, 110, 3330-3335 (2006).

Safarov, J., Millero, F. J., Feistel, R., Heintz, A., Hassel, E., Thermodynamic properties of standard seawater: Extensions to high temperatures and pressures. Ocean Science, 5, 235-246 (2009).

Safarov, J., Hamidova, R., Zepik, S., Schmidt, H., Kul, I., Shahverdiyev, A., Hassel, E., Thermophysical properties of 1-hexyl-3-methylimidazolium bis(trifluoromethylsulfonyl) imide at high temperatures and pressures. Journal of Molecular Liquids, 187, 137-156 (2013).

Segovia, J. J., Fandiño, O., López, E. R., Lugoa, L., Martín, M. C., Fernández, J., Automated densimetric system: Measurements and uncertainties for compressed fluids. The Journal of Chemical Thermodynamics, 41, 632-638 (2009).

Shimizu, Y., Ohte, Y., Yamamura, Y., Saito, K., Effects of thermal history on thermal anomaly in solid of ionic liquid compound, $[C_4mim][Tf_2N]$. Chemistry Letters, 36, 1484-1485 (2007).

Stabinger, H., Density Measurement Using Modern Oscillating Transducers. South Yorkshire Trading Standards Unit, Sheffield (1994).

Tokuda, H., Hayamizu, K., Ishii, K., Susan, Md. A. B. H., Watanabe, M., Physicochemical properties and structures of room temperature ionic liquids. 2. Variation of alkyl chain length in imidazolium cation. Journal of Physical Chemistry B, 109, 6103-6110 (2005).

Tokuda, H., Tsuzuki, S., Susan, Md. A. B. H., Hayamizu, K., Watanabe, M., How ionic are room-temperature ionic liquids? An indicator of the physicochemical properties. Journal of Physical Chemistry B, 110, 19593-19600 (2006).

Troncoso, J., Cerdeiriña, C. A., Sanmamed, Y. A., Romaní, L., Rebelo, L. P. N., Thermodynamic properties of imidazolium-based ionic liquids: Densities, heat capacities, and enthalpies of fusion of [bmim][PF_6] and [bmim][NTf_2]. Journal of Chemical & Engineering Data, 51, 1856-1859 (2006).

Valkenburg, M. E. V., Vaughn, R. L., Williams, M., Wilkes, J. S., Thermochemistry of ionic liquid heat-transfer fluids. Thermochimica Acta, 425, 181-188 (2005).

Vranes, M., Dozic, S., Djeric, V., Gadzuric, S., Physicochemical characterization of 1-butyl-3-methylimidazolium and 1-butyl-1-methylpyrrolidinium bis(trifluoromethylsulfonyl)imide. Journal of Chemical & Engineering Data, 57, 1072-1077 (2012).

Wandschneider, A., Lehmann, J. K., Heintz, A., Surface tension and density of pure ionic liquids and some binary mixtures with 1-propanol and 1-butanol. Journal of Chemical & Engineering Data, 53, 596-599 (2008).

Wu, B., Reddy, R. G., Rogers, R. D., Novel ionic liquid thermal storage for solar thermal electric power systems. Proceedings of Solar Forum 2001 Solar Energy: The Power to Choose, Washington, DC, April 22 (2001).